International Journal of Hydrogen Energy 66 (2024) 468–478

Contents lists available at ScienceDirect

International Journal of Hydrogen Energy

journal homepage: www.elsevier.com/locate/he

Natural isotope fingerprinting of produced hydrogen and its potential applications to the hydrogen economy

J.J. Gibson [a,*], P. Eby [a], A. Jaggi [b]

[a] InnoTech Alberta, 3-4476 Markham Street, Victoria, BC V8Z 7X8, Canada
[b] InnoTech Alberta, 3608 – 33 Street NW, Calgary, Alberta T2L 2A6, Canada

ARTICLE INFO

Handling Editor: Mehran Rezaei

Keywords:
Isotopes
Deuterium
Hydrogen
Electrolysis
Biohydrogen
Fossil fuel conversion

ABSTRACT

Stable isotopes of hydrogen ($^2H/^1H$) carry natural fingerprints of produced hydrogen by mode of origin which are difficult or costly to adulterate. A newly compiled database of 5677 measurements reveals that *green* hydrogen (electrolytic or biological hydrogen, e.g., nitrogenase, hydrogenase) is readily distinguished by its considerable depletion in heavy isotopic species, ranging from −831 to −555 ‰ in δ^2H relative to Vienna Standard Mean Ocean Water (V-SMOW), as compared to −377 to +196 ‰ for fossil fuel sources (*grey/turquoise* hydrogen), and −379 to 0 ‰ for wood/biomass burning (*brown* hydrogen), compared to analytical uncertainty of close to ±1 ‰. *White* hydrogen, naturally produced in a variety of geologic settings, ranges from −996 to −49 ‰, reflecting diverse overlapping origins. Potential applications of fingerprinting include tracking of produced hydrogen by source, process and distribution control, grading and regulation of low carbon intensity (CI) products, and leakage detection for carbon storage operations.

1. Introduction

Hydrogen is a promising renewable, clean fuel for use in combustion engines and fuel-cell electric vehicles, which has led to significant recent interest in its efficient commercial production [1]. Hydrogen demand worldwide has increased from an estimated 30 million tonnes per year in 1985, when it was mainly used in the Haber-Bosch process for producing ammonia fertilizer [2], to over 95 million tonnes per year today [3]. Although the majority of industrial hydrogen is produced using fossil fuels, carbon capture utilization and storage (CCUS) strategies are under development to mitigate the impact of greenhouse gas emissions as the cornerstone of many regional and national strategies to transition to the hydrogen economy [[4,5]]. Requirements are also being developed for greenhouse gas reporting by applicable facilities including hydrogen production and other source categories [6], and development of clean hydrogen standards [7]. While deployment of hydrogen is in the early stages across many jurisdictions in Canada, harmonization of codes and standards across provincial and international markets through efforts such as the Canada/U.S. Regulatory Cooperation Council are acknowledged to be important to ensure best practices are followed [[5], p.98]. Worldwide standards are also an important focus of many of the developing economies of the world [8]. Development of technologies that support origin and source tracking, process and distribution control, identification and grading of low carbon intensity (CI) products, leakage detection and CCUS efficiency will clearly be important for such regulatory purposes.

Isotopes of hydrogen, although used routinely in the nuclear industry, for forensic and drug investigations [[9,10]], for food authentication and adulteration studies [[11,12]], and for a wide variety of applications in the fields of water resources, geology, ecosystems and atmospheric studies [[13–17]], have not been widely discussed as a potential technology or regulatory tool applicable to the hydrogen economy. Hydrogen has three principal isotopes, two of which are stable (protium, ^1H and deuterium, ^2H) and the third being radioactive (tritium, ^3H). Although deuterium makes up only 150 parts per million (ppm) of naturally occurring hydrogen, for decades it has been separated from natural water to isolate “heavy water” for use as a moderator for slow neutrons in fission reactors [18]. Likewise, deuterium and tritium are relied upon for the most efficient state-of-the-art fusion reactors which aim to generate abundant energy by fusing deuterium and tritium to form helium. Separation of the isotopes of hydrogen is often carried out using cryogenic distillation, thermal diffusion, centrifugation, catalytic exchange or water electrolysis [19]. Deuterium enrichment by electrolysis has long been known and utilized for heavy water

* Corresponding author.
E-mail address: john.gibson@innotechalberta.ca (J.J. Gibson).

https://doi.org/10.1016/j.ijhydene.2024.04.077
Received 20 January 2024; Received in revised form 7 March 2024; Accepted 5 April 2024

production since the 1930s, as well as for hydrogen production, and relies on splitting water into O_2 and H_2.

Methods for hydrogen production are numerous (Table 1) and span a range of CI. Some production methods such as electrolysis using renewable energy sources have been standardly referred to as *green hydrogen*. While we are not explicitly advocating its use, the concept of a hydrogen colour spectrum has recently become popular as a means of classifying and categorizing the wide range of production methods used to produce hydrogen and their carbon intensities [25]. We use the colour spectrum here as a reference for purposes of discussing variations in production methods and the nature of isotopic fingerprinting. *Green* hydrogen or 'clean hydrogen' is generally defined as being derived from renewables; *pink* hydrogen is produced by electrolysis using nuclear power; *red* hydrogen is produced by thermochemical splitting using nuclear power; *purple* hydrogen is a combination of *pink* and *red* hydrogen; *yellow* hydrogen is produced using grid power of mixed origin; *grey* hydrogen denotes hydrogen produced from natural gas, oil or bitumen through steam methane reforming (SMR), partial oxidation, or autothermal reforming (ATR); *turquoise* hydrogen is produced by methane pyrolysis yielding solid carbon as a byproduct; *brown* hydrogen and *black* hydrogen are produced from gasification of lignite and bituminous coal, respectively; *blue* hydrogen is produced from fossil fuels but with carbon capture, utilization and storage to reduce GHGs; *aqua* hydrogen is produced in the ground from bitumen or oil through SMR to produce syngas, with subsequent collection of hydrogen gas through membranes in the production wells [26]; *white* hydrogen is natural hydrogen occurring as a free gas present in rock formations and hydrothermal fluids in a wide range of geologic settings. Note that hydrogen produced from biomass waste by combustion is often deemed *brown* hydrogen, although we differentiate and classify biohydrogen reactions such as nitrogen fixation, regulated by *nitrogenase* enzymes, involving reduction of N_2 to NH_3, and *hydrogenase* enzymes, involving splitting of water into O_2 and H^+, as 'clean hydrogen' [24] or *green* hydrogen. Photocatalysis is likewise considered *green* hydrogen as it uses only solar energy to split water molecules. According to the hydrogen spectrum concept, the combination of energy source, production technology and GHG mitigation technologies employed determines the final colour classification (see Fig. 1).

Table 1
Hydrogen production methods and general reactions (from Ref. [1], unless otherwise stated).

Method	Description	H-Spectrum Colour[a]	Reactions
Steam methane reforming (SMR)	Methane-steam reaction at high pressure over catalyst at 700°–1000 °C, 15–40 atm	*grey*	$CH_4 + H_2O \leftrightarrow CO + 3H_2$
Partial oxidation	Catalytic or noncatalytic combustion of hydrocarbon with limited O_2 at 1200–1500 °C, 20–150 atm	*grey*	$CH_4 + ½O_2 \rightarrow CO + 2H_2$
Gasification	Coal converted to syngas and hydrogen, 700–1200 °C, 40–100 atm	*black, brown*	$3C + O_2 + H_2O \rightarrow 3CO + H_2$
Water-gas shift [20]	Carbon monoxide and steam reacted using catalyst to produce CO_2 and H_2 at 400–900 °C, 0–85 atm; often used to adjust H_2/CO ratios following SMR, POX, Gasification	*grey*	$CO + H_2O \leftrightarrow CO_2 + H_2$
Cracking [21]	Thermal or catalytic decomposition of alkanes at 450–750 °C, 50–70 atm	*grey*	$CH_4 \rightarrow C_{(s)} + 2H_2$
Pyrolysis [[22,23]]	Anaerobic reaction producing solid carbon byproduct at 500–1200 °C, low P	*turquoise*	$CH_4 \rightarrow C_{(s)} + 2H_2$
Biohydrogen reaction [24]	Bacterial and microalgal production using sunlight or organic matter.	*green*	e.g., $N_2 + 8H^+ + 8e^- \rightarrow 2NH_3 + H_2$; $2H^+ + 2e^- \leftrightarrow H_2$
Electrolysis	Use of an electrolyzer to dissociate water	*green, pink, yellow*	$H_2O \rightarrow H_2 + ½O_2$
Thermochemical water splitting	Requires temperatures of 2500 °C	*red, purple*	$H_2O \rightarrow H_2 + ½O_2$
Photocatalysis	Reduction of water to hydrogen over semiconductor catalyst	*green*	$H_2O \rightarrow H_2 + ½O_2$

[a] Note that H-spectrum colours are used as a reference only. Also note that grey hydrogen can be transformed to *blue*, *turquoise* or *aqua* hydrogen by CCUS.

To give some idea of the most common methods in use and their relative importance, we provide plots showing North American production data obtained from the International Energy Agency [3] (Fig. 2). They provide an overview of 31 commercial hydrogen producers, 19 of which are producing green hydrogen by electrolysis (alkaline exchange membrane; AEM) or proton exchange membrane; PEM), 2 producing *brown* hydrogen from biomass, and 9 producing hydrogen from fossil fuels, the latter of which are licenced conditional on employing CCUS technologies for greenhouse gas (GHG) mitigation, and 1 plant producing hydrogen from methane pyrolysis. While there appears to be considerable interest in green methods, the vast majority of the production capacity remains dominated by fossil fuel sources. End uses of produced hydrogen include refining, ammonia, commercial gases, mobility, power and CH_4 grid injection.

This paper describes a newly compiled database of 5677 hydrogen isotope measurements from relevant hydrogen studies presented in the peer reviewed literature, as well as a limited amount of relevant new experimental data, that sheds light on the potential value of isotopes for fingerprinting produced hydrogen. Prior to conducting the literature survey and experimental work, and based on our considerable experience with isotopes in water and environmental studies, our hypothesis was that hydrogen isotopes had great potential to be used as a tool for understanding and labelling produced hydrogen. Given that H_2 is the second most abundant reactive trace gas in the atmosphere next to CH_4 [27], we anticipated that there was likely enough data already published on the range of mechanisms of H_2 production available from natural experiments and/or anthropogenic source studies, including global inventories, to demonstrate the effect of isotope labelling by various mechanism of production. The main objective of this paper is to provide an overview of our results in the context of the ability of isotopes to fingerprint produced hydrogen, and to discuss some of the main applications we foresee as well as gaps and challenges that might be encountered.

2. Methods

2.1. Experimental

Several experiments were conducted at InnoTech Alberta, Calgary to compliment the literature review and to provide better understanding of the stability, repeatability and robustness of isotopic signatures for labelling hydrogen production sources. Initial trials of various commercially available benchtop hydrogen production lines were operated and sampled including both AEM and PEM electrolysis systems, and a methane pyrolysis line, the latter similar to that of Dolgikh et al. [28].

The alkaline electrolyzer used was a 5 cm^2 AEM water electrolyzer purchased from Dioxide Materials™ (1100 Holland Dr. Boca Raton, FL, 33487-2701, USA) employing a 1 M KOH solution and a Sustainion® anion exchange membrane similar to that utilized by Liu et al. [29]. The PEM electrolyzer was a Titan EZ-500 2-layer cell stack purchased from the Fuel Cell Store (1 W Bronze Ln, Bryan Tx 77807, USA). The PEM utilized HPLC or DI waters with electrical conductivity ranging from 1.92 to 2.14 μS/cm. Individual trials were run for 30–40 min to allow for

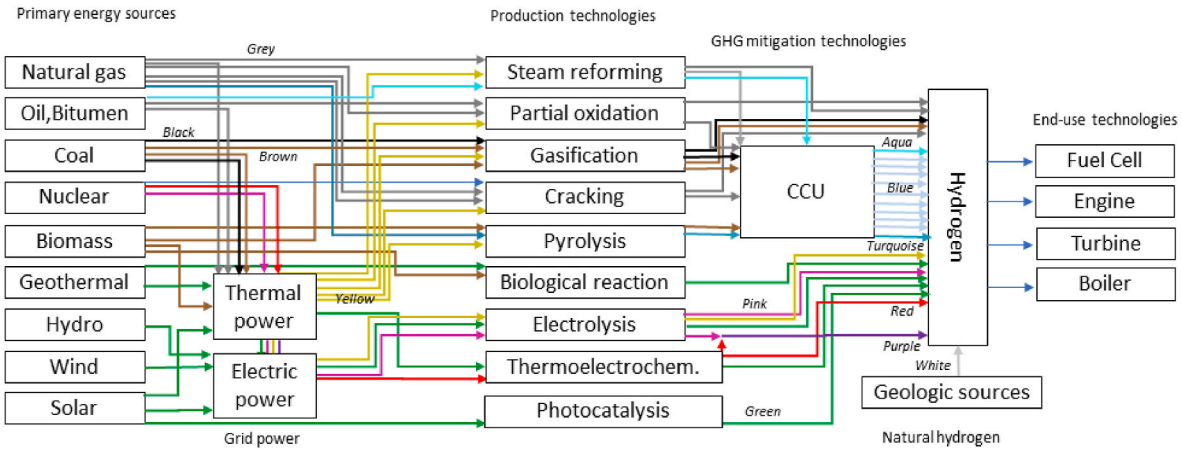

Fig. 1. (Colour) Schematic flow chart showing energy sources, production technologies and end uses of produced hydrogen (after [1]), labelled according to hydrogen spectrum [25]. CCUS transforms *grey*, *brown* or *black* hydrogen sources to *blue*, *turquoise* and *aqua*. Note that *white* hydrogen refers to natural sources of hydrogen from geologic sources. See text for description. (For interpretation of the references to colour in this figure legend, the reader is referred to the Web version of this article.)

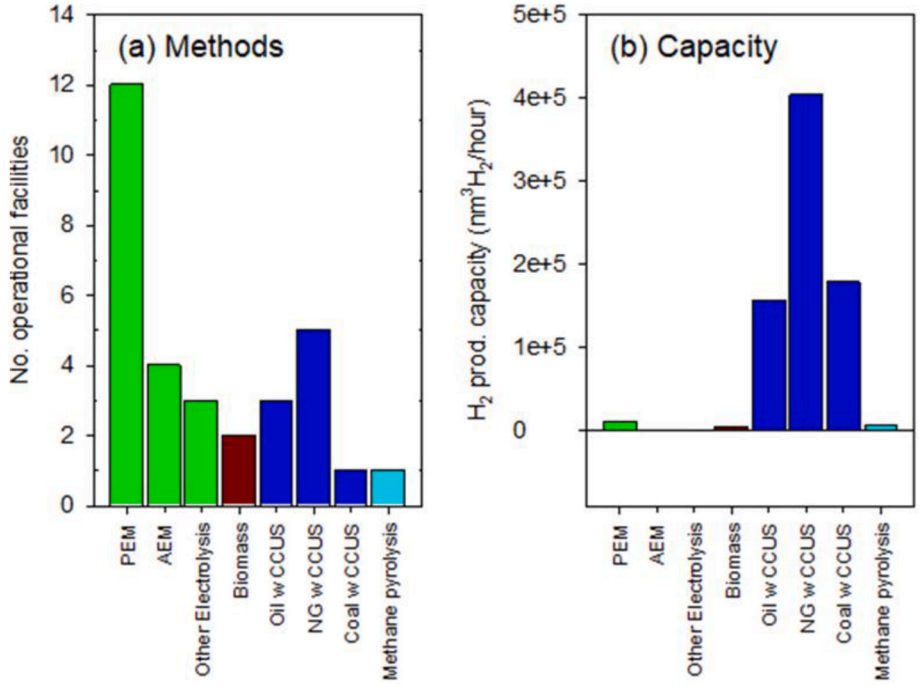

Fig. 2. (Colour) Summary of operational hydrogen production in North America, including: (a) production method; (b) IEA normalized capacity [3]. Colours reflect hydrogen spectrum classifications (see text for discussion). (For interpretation of the references to colour in this figure legend, the reader is referred to the Web version of this article.)

sufficient H_2 production to allow analysis on the isotope ratio mass spectrometer.

Additional H_2 samples and source waters were also obtained from a commercially operated electrolysis system and an SMR system. Produced hydrogen was collected in double-ended 150 mL steel cylinders (Swagelok®, 304L-HDF4-150), each with two needle valves (Swagelok®, SS-1RM4-F4). Occasionally the vessels were found to have leaked during shipping, so these results were repeated where possible. In addition, commercially available lecture bottles of pure H_2 were also sourced and analyzed.

Isotope determinations on hydrogen gas and methane were made using a Thermo Scientific MAT253 isotope ratio mass spectrometer fitted with a Conflo IV interface, Trace GC Ultra, and GC Isolink. Gas samples were introduced onto a Molsieve 5A PLOT column (0.32 mm ID, 30 m) using a Valco 6-port valve and sample loop. After chromatographic separation, components pass through a water trap before passing to the Conflo interface. No pyrolysis interface is required. In-house standards of known isotopic composition were also run to allow calibration to the V-SMOW scale. Isotope determinations on water were made using a Thermo Scientific Delta V Advantage isotope ratio mass spectrometer with HDevice [30]. Results are reported in δ notation in permil (‰) relative to V-SMOW:

$$\delta^2 H\ (‰) = \left(\frac{R_{sample}}{R_{V-SMOW}} - 1\right) \times 1000$$

and normalized to the SMOW-SLAP scale, where SLAP is Standard Light Arctic Precipitation [31]. Analytical uncertainty (1σ) was estimated to be ±0.937 ‰ based on the standard deviation of 44 repeat

measurements, which is better than the nominally reported long-term uncertainty for measurement of deuterium in the lab (±1 ‰).

2.2. Literature review

A total of 1830 peer-reviewed papers reporting on hydrogen produced in nature, experimental investigations, or arising from unintended or anthropogenic causes were reviewed. Those containing relevant hydrogen isotope measurements were extracted and results were compiled in a database. The most interesting results were gleaned from studies on global atmospheric inventories or budgets that apportioned atmospheric H_2 according to its sources, which ably demonstrated isotopic differentiation. The overall dataset, provided as *Supplemental Material*, also contains related data on inventories of reactants, intermediates, as well as source water and ambient atmospheric data for the troposphere and stratosphere. Meteoric water data were obtained from the International Atomic Energy Agency's (IAEA) Global Network for Isotopes in Precipitation (GNIP) available online [32]. Estimates of δ^2H in atmospheric water vapour for GNIP stations was obtained from Gibson et al. [33]. In total, 5677 hydrogen isotope results are reported in the database including precipitation (4669), atmospheric moisture (499), molecular hydrogen (355), and other intermediates/precursors (154).

3. Results and discussion

3.1. Experimental results

Electrolytic hydrogen from the on-site experiments was found to range from −682 to −766 ‰ in δ^2H including both AEM and PEM trials (Table 2). In all but one experiment it was found that the fractionation between source water and hydrogen ranged between −600 and −676 ‰, which is similar to that calculated for hydrogen ions at equilibrium with water [34]. The only anomaly was for the first trial where the apparent fractionation was only −536 ‰, although we were somewhat unfamiliar with the apparatus and may have had some difficulty with sampling the H_2 without minor leakage. In all experiments, we also observed significant enrichment of water in the hydrogen cell near the cathode (−) and only minor enrichment in water near the anode. Analysis of both $\delta^{18}O$ and δ^2H in these waters confirmed that the waters were enriching along slopes ranging between 10 and 20 in $\delta^{18}O$-δ^2H space, steeper than the Global Meteoric Water Line (see Ref. [33]), and much steeper than a simple evaporation trend which is typically in the range of 5–6. The one PEM trial that was carried out off-site by a commercial facility operator, and that was not under our direct supervision, yielded a confounding result. In this single trial, source water was found to be nearly identical to the produced H_2 (−69.3 versus −71 ‰, respectively) such that the apparent fractionation was positive and subdued (+1.7 ‰). Because this is clearly an anomalous result within the context of our 19 other electrolysis trials where mean apparent fractionation was −608 (±35) ‰, and we were unable to verify experimental conditions or details of the apparatus configuration, we decided to set this result aside in our statistical treatment of the overall survey results. However, we do note this finding and recommend that it be further investigated.

The other off-site method trialed was SMR. We presume that the apparatus was similar to that described by Spagnolo et al. [35] but without a catalyst reactor bed for deuterium oxide (D_2O) production. Source water for the system was measured to be −61.7 ‰. Only one trial was possible with the on-site methane pyrolysis apparatus as trained staff to operate it had limited free time available when the experiments were being run. Precursor methane for the trial was unfortunately not provided, although produced H_2 was measured to be −181 ‰ in δ^2H, which is in the range of values noted in the literature survey. The methane pyrolysis method run on-site yielded hydrogen measured at −19.0 ‰ in δ^2H. This is consistent with other methane-derived hydrogen sources that we noted from the literature, as presented later. One interesting finding was that the conversion of methane to H_2 and carbon black was only partial, such that a residual methane of −83 ‰ remained, as compared to a precursor methane of −62‰, which is consistent with the produced H_2 being enriched by +43 ‰. Hydrogen samples in lecture bottles or tanks were also obtained from several

Table 2
Summary of experimental results for this study. δ^2H results in ‰ V-SMOW.

Apparatus	Type	Volts/Amps	Source water	Anode water	Cathode water	Produced H_2	1 σ	Apparent fractionation	n
			‰ V-SMOW						
Electrolysis	AEM	−/−	−146	−139	–	−682	1.53	−536.0	3
		2.2/1.5–3	−133.2	−134.1	−140.6	−754	0.77	−620.8	2
Electrolysis	PEM	−/−	−141.7	−146	–	−766	2.52	−624.3	2
		−/−	−146	–	−141.7	−766	–	−620.0	1
		3.8/16–20.4	−150.8	−97	−147	−757	0.62	−606.2	3
		3.9/15–16.5	−150.3	−98	−143	−758	0.66	−607.7	3
		3.9/15-16	−150.3	−90.3	−143.5	−758	0.71	−607.8	3
		3.9/16–16.4	−150.2	−89.5	−143.5	−758	0.47	−599.7	3
		3.8/15.8–16	−150.3	−91.6	−143.6	−750	0.91	−669.9	3
		3.9-4/18–18.4	−68.1	−33.3	−64.9	−738	2.26	−671.2	3
		3.9-4/18–18.2	−67.8	−13.3	−61.8	−739	0.36	−673.4	3
		3.8-3.9/16–18.1	−67.6	−4.6	−63.2	−741	0.55	−675.8	3
		3.8-3.9/15.5–17	−67.2	−2.4	−62.5	−743	1.34	−675.0	3
		3.9/14.4–15.5	−72.0	−8.1	−69.7	−747	0.76	−675.4	3
		3.9/14.3-14.8	−72.6	−8.1	−69.2	−748	1.53	−674.7	3
		3.9/14–14.3	−73.3	−8.1	−69.4	−748	0.84	−674.9	3
		3.9/14–14.3	−73.1	−8.8	−68.5	−748	1.15	−673.5	3
		3.9/14.74	−73.5	−7.7	−68.3	−747	1.13	−607.7	3
Electrolysis[a]	PEM	−/−	−69.3	–	–	−71.0	0.82	+1.7	3
Steam methane reforming[a]			−61.7	n.a	n.a.	−181	1.13	−119.3	3
Methane Pyrolysis[b]						−19.0	0.91	+43.0	2
Lecture Bottles/Tanks	Supplier A					−560	1.15		3
	Supplier B					−293	0.58		3
	Supplier C					−160	0.58		4
	Supplier D					−359	0.58		3

[c]Source methane n.a. not applicable.
[a] Offsite commercial apparatus, supplier confidential.
[b] Onsite experiment – methane feedstock (−62 ± 1.6 ‰, n = 2), product methane (−83 ± 1.5 ‰, n = 2).

confidential suppliers and analyzed to determine the δ^2H values (Table 2). The values ranged from −160 to −560 ‰, although details on production methods were not provided, and it was not clear if the gases were blended from more than one production source. We have been informed that blending of feedstock from different production facilities is standard practice in the commercial gas business to offer a range of isotopic compositions or other gas properties. Overall, the observed range of δ^2H compositions appears consistent with a mixture of electrolysis and fossil fuel derived product.

3.2. Literature review

Important contributions to general understanding of the deuterium isotope effects [[36,37]] and isotopic fractionation in methane-hydrogen-water systems [[34,38]] have been known and utilized for some time. While only a single paper was found that reported hydrogen isotope data for source water, methane and produced H_2 from an operating, commercial hydrogen production facility [35], there is a significant body of literature that reports isotopic data from heavy water enrichment experiments investigating various methods and catalysts (e.g., Refs. [2,39–46]) as well as theoretical calculations of $^2H/^1H$ isotope effects [[47,48]]. Production of heavy water serves an important role in the nuclear industry, which has led to study and refinement of a number of heavy isotope separation processes including water distillation, electrolysis, hydrogen-sulfide water exchange, hydrogen distillation, monothermal and bithermal ammonia-hydrogen exchange and steam-hydrogen exchange [49]. Non-nuclear use of deuterium includes production of advanced electronics, deuterated solvents, deuterated pharmaceuticals, hydrogen arc-lamps, neutron generators, and tracers in hydrological, biological, and medical studies [50]. Scientific investigations have applied isotopic tracers, mainly artificially introduced deuterated water, to evaluate catalysts and/or reaction mechanisms in various reforming processes involving H_2 production. Some examples include studies of reaction mechanisms associated with partial oxidation of methane to syngas [[19,51,52]], PEM fuel cell operations [[41,53]], water-hydrocarbon reaction mechanisms associated with pyrolysis [[54,55]], and hydrogen production kinetics in steelmaking [56]. This is by no means an exhaustive list of isotopic studies, but a comprehensive review is somewhat tangential to the purpose of this paper which is to highlight fingerprinting of produced hydrogen.

Despite limited data on commercial hydrogen production, we discovered that there is a wealth of relevant information including isotopic investigations that have characterized hydrogen produced by natural and anthropogenic processes that can be applied as analogues for various methods of industrial production. Measurement of deuterium variations in atmospheric hydrogen (e.g. Refs. [57,58]) and efforts to understand the atmospheric hydrogen cycle [59–61] offer important insights into the isotopic signatures of hydrogen produced through wood and biomass combustion [62], fossil fuel combustion [63], car exhaust [64], photochemical oxidation of methane and volatile organic carbon [65–69], nitrogen fixation from the oceans and land [61,70], nitrogenase, hydrogenase and/or cyanobacterial production [24,70–72], and biogas production [70]. Many of these studies have sought to close the atmospheric budget by improving the mechanistic understanding of tropospheric and extreme stratospheric enrichment of deuterium [74,75] as well as natural regulatory processes such as the scavenging of H_2 by enzymes in soils [59,76] and by OH radicals in the atmosphere [74]. Efforts have also been made to understand both biogenic occurrences of H_2 in groundwater [76] and natural, *white* hydrogen, in a range of geologic settings [17,77–79]. Clumped isotopic methods for natural abundance variations of H_2 have also been developed offering great potential for future fingerprinting refinements (e.g., Refs. [80,81]). By examining the systematic isotopic fractionation between reactants, intermediates, and hydrogen products, we are able to provide a first assessment of anticipated signatures that would accompany many of the proposed or operation industrial production of hydrogen, and in doing so establish that there are likely to be important differentiable isotopic fingerprints imparted to various components of the produced hydrogen spectra.

3.3. Combined survey

Results from the literature review combined with new experimental results (Table 2) provide a robust perspective of distinct labelling of produced hydrogen according to the process associated with its formation (Fig. 3a). Note that hydrogen isotope data for reactants, intermediates and ambient environmental hydrogen (Fig. 3a) was also collected to assess the isotopic composition of hydrogen-bearing compounds in the precursors and, hence, to allow estimation of the isotopic separation between specific reactants and produced hydrogen product, which is important for evaluating and understanding individual fractionation processes in detail. As a first illustration of the hydrogen fingerprinting effects we will first describe the broad-scale differences observed in the signatures of produced hydrogen (Fig. 3a) and then we will proceed to discuss some of the specific fractionation mechanisms to the degree they are understood or can be predicted based on existing evidence. A database of combined results from the literature review and experimental data is provided as Supplementary Material. Descriptive statistics and references are provided both for hydrogen gas (Table 3) and precursors (Table 4).

3.4. Hydrogen fingerprinting

The most striking feature of the survey is that *green* hydrogen products, i.e. H_2 produced by nitrogen fixation, nitrogenase/hydrogenase enzymes, from biogas, and from water-splitting reactions such as electrolysis, are distinctly more depleted in deuterium as compared to *grey* hydrogen produced by fossil fuel conversion, including methane pyrolysis and methane steam reformation, as well as hydrogen produced unintentionally or anthropogenically through the relatively inefficient processes of incomplete combustion (i.e., fossil fuel combustion, biomass combustion, wood burning, and car exhaust). Hydrogen produced naturally in the atmosphere through methane oxidation and VOC oxidation, which might be considered as useful low-pressure analogues for reforming by partial oxidation, are also shown to be distinct from *green* hydrogen, and are found to be enriched relative to other fossil fuel derived hydrogen products. *White* hydrogen, because it occurs naturally in a range of geologic settings, expectedly spans a wide range of sources and broadly overlaps both *green* and *grey/turquoise* hydrogen sources. *White* hydrogen has been found to occur in relation to mantle sources, hydrothermal activity, radiolytic alteration and serpentinization, fault-zones, mid-ocean ridge spreading, continental volcanic activity, kimberlites and bacterial activity [[17,82]]. The range observed for *white* hydrogen is largely consistent with the known range of deuterium content between the oceans ($\delta^2H \sim 0$ ‰) and the mantle ($\delta^2H = <-218$ ‰) [83], and in primary minerals formed within the early solar system ($\delta^2H \sim -850$ ‰; [84]). The fact that *white* hydrogen overlaps with *green* hydrogen may be evidence of bacterially mediated geological processes in some settings. Furthermore, overlap with *green* hydrogen is not likely to pose a dilemma for fingerprinting as *white* hydrogen is also essentially "*green*" as it does not contribute to anthropogenic GHG emissions.

Apart from one anomalous experimental result mentioned previously and to be justified later on, hydrogen isotope values ranged from −831 to −555 ‰ for *green* hydrogen, −377 to +196 ‰ for all *grey* hydrogen including fossil fuel burning, oxidation reactions and car exhaust, −379 to 0 ‰ for *brown* hydrogen including wood/biomass burning, and −996 to −49 ‰ for *white* hydrogen. As a significant gap of 178 ‰ exists between *green* and *grey* hydrogen, there appears to be significant potential for isotopes to be used as a natural fingerprinting tool to distinguish these sources. However, there is relatively little isotopic distinction between *grey* and *brown* hydrogen. As noted by Luo et al. [71], the significant depletion in hydrogen produced through bacterial activity or

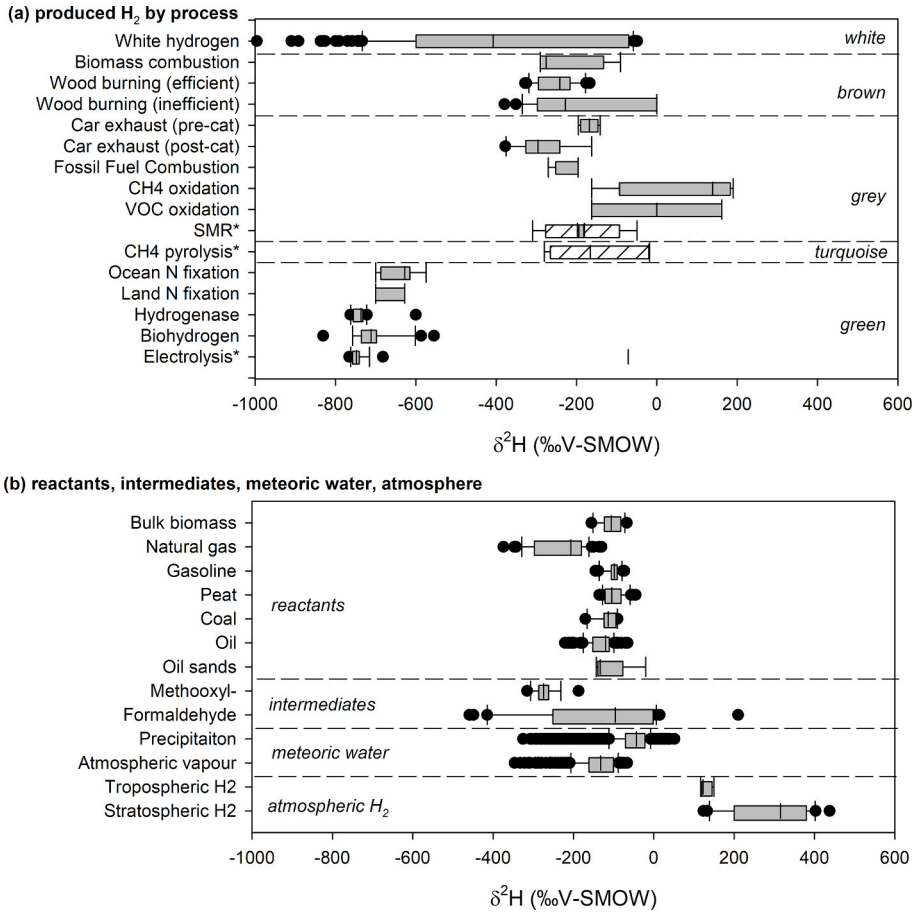

Fig. 3. Compilations of (a) hydrogen isotope data for produced hydrogen by production process. * denotes incorporation of new experimental data; cross-hatching indicates calculated ranges based on isotope characteristics of hydrogen-bearing compounds in precursors, and (b) published hydrogen isotope data for common precursors/reactants, intermediates and ambient environmental H_2 in the troposphere and stratosphere. Boxes display 25th and 75th percentiles whereas whiskers display 10th and 90th percentiles; lines display median values and closed circles show outliers. See Tables 3 and 4 for numerical statistics and references.

electrolysis arises from splitting of the water molecule itself as compared to fossil fuel or biomass conversion, the latter of which involves a less energetic release of carbon-bound hydrogen. It is important to distinguish between biogas (*brown* hydrogen) and biohydrogen (*green* hydrogen), the former involving conversion of organics to CH_4 and then H_2, while the latter involves conversion of water and organics directly to H_2 as mediated by *nitrogenase* or *hydrogenase* enzymes.

3.5. Source labeling

Hydrogen isotope data were gathered for a variety of carbon sources relied upon for hydrogen production including bulk biomass, natural gas, gasoline, peat, coal, oil, and oil sands bitumen (Fig. 3b). Ranges established from the literature review were as follows: bulk biomass (−155 to −67 ‰), natural gas (−374 to −130 ‰), gasoline (−145 to −73 ‰), peat (−135 to −45 ‰), coal (−170 to −190 ‰), oil (−221 to −65 ‰) and oil sands bitumen (−143 to −20 ‰). References and additional statistics are provided in Table 4. Among the fossil fuels, natural gas extends to a more negative range as it is known to be highly reactive with soils and rock mass, and may include both thermogenic and biogenic types, the latter being strongly affected by bacterial transformation of CO_2 to methane [93]. For freshwater systems, Douglas et al. [96] confirmed that the isotopic signature of hydrogen from water is the strongest determinant of the isotopic signature of hydrogen in methane, although methane oxidation, methanogenesis pathways, and other biogeochemical variables are also important. Water and/or atmospheric water vapour sources are also influential for some hydrogen production reactions, particularly SMR, and the water splitting reactions which include electrolysis, thermochemical, and photocatalysis methods. For our assessment, variation in δ^2H for water was estimated from ranges of δ^2H in monthly mean precipitation based several hundred stations in GNIP [32]. δ^2H in atmospheric moisture was estimated from GNIP data using an approximation that accounted for climate and seasonality, and that has been shown to accurately predict isotopic enrichment patterns in lakes and soils [33].

3.6. Fossil fuel conversion

In terms of industrial hydrogen production, the most commonly used process is currently SMR whereby methane is reacted with steam at high temperatures to produce water and carbon dioxide [105]. Partial oxidation has also been used either as a separate method or in combination with SMR, the latter often referred to as Autothermal reforming (ATR). ATR is recognized for its ability to capture CO_2 more easily, for its simpler, more compact design than SMR and lower water demand [105]. Gasification of coal or other hydrocarbons is a much older method that is still in use in North America and elsewhere to produce hydrogen [3]. H_2 production by these methods is often augmented by secondary processing using the water-gas shift reaction to enhance H_2 yields from syngas ($CO + H_2$) [20].

Combined, these reactions tend to produce H_2 which carries the isotopic signatures of the reactants, commonly CH_4 and H_2O, and therefore are expected to yield H_2 with isotopic signatures intermediate between these reactants (see Ref. [35]). In contrast, methods such as

Table 3
Compiled statistics for isotope composition of hydrogen gas by origin.

Hydrogen type	n	Mean	Std Dev	Range	Max	Min	Median
	δ^2H (‰ V-SMOW)						
White hydrogen	152	−385	269	947	−49	−996	−408
Biomass combustion	4	−233	96	200	−90	−290	−275
Wood burning							
Efficient	24	−249	47	161	−167	−328	−241
Inefficient	24	−176	145	379	0	−379	−227
Car exhaust							
pre-catalytic	4	−168	22	54	−141	−195	−168
post-catalytic	17	−285	69	215	−162	−377	−296
Fossil fuel combustion	4	−215	37	74	−196	−270	−196
CH_4 oxidation	4	77	162	352	190	−162	139
VOC oxidation	2	0	229	324	162	−162	0
Steam methane reform	8	−183	94	260	−49	−309	−182
CH_4 pyrolysis	6	−151	113	262	−18	−280	−165
Ocean N fix	6	−640	45	125	−575	−700	−628
Land N fix	3	−652	42	72	−628	−700	−628
Hydrogenase	20	−735	34	163	−600	−763	−737
Biohydrogen plant	22	−706	57	276	−555	−831	−712
Electrolysis	15	−746	19	84	−682	−766	−748

Sources: *White* hydrogen [17,77–79,82–92]; Biomass combustion [59,61,62,75]; Wood burning [62]; Car exhaust [64]; Fossil fuel combustion [59,61,62,75]; CH4 oxidation [59,61,62,75]; VOC oxidation [61,62]; Steam methane reform: Experimental, this study; limits calculated from range of precipitation data of IAEA [32] and range of methane data of Schoell [93]; Pyrolysis: Experimental; limits calculated from range of methane data of Schoell [93]; Ocean N fix [59,61,62,75,94]; Land N fix [59,62,75]; Hydrogenase [71,72]; Biohydrogen plant [70]; Electrolysis Experimental, this study

Table 4
Compiled statistics for isotope composition of hydrogen-bearing compounds in reactants, intermediates, meteoric water, atmospheric waters.

Source	N	Mean	Std Dev	Range	Max	Min	Median
	δ^2H (‰ V-SMOW)						
Biomass bulk	36	−105	26	88	−67	−155	−106
Natural gas	47	−229	67	244	−130	−374	−206
Gasoline	25	−102	19	72	−73	−145	−98
Peat	86	−98	25	90	−45	−135	−104
Coal	10	−115	23	80	−90	−170	−114
Oil	137	−130	31	156	−65	−221	−120
Oil sands	5	−113	52	123	−20	−143	−133
Atmos. methoxyl radical	26	−270	30	128	−187	−315	−274
Atmos. formaldehyde	32	−139	164	669	210	−459	−96
Precipitation	4163	−54	48	377	52	−325	−43
Atmos. moisture	299	−140	53	280	−66	−346	−132
Atmos. H_2	6	129	14	33	150	117	123
Stratospheric H_2	22	287	100	314	438	124	316

Sources: Biomass bulk [62]; Natural gas [82,93,95,96]; Gasoline [97]; Peat [98,99]; Coal [100]; Oil [101,102]; Oil sands [103]; Methoxyl- [62]; Formaldehyde [60,69]; Precipitation [32]; Atmos. Moisture [33]; Atmospheric H_2 [58,104]; Stratospheric H_2 [57].

cracking and pyrolysis, or dry reforming, all reactions which do not involve significant amounts of water, would be expected to produce H_2 that is more reflective of the methane source. In fact, techniques such as pyrolysis are relied upon in isotope ratio mass spectrometry for quantitative conversion of hydrocarbons to H_2 for hydrogen isotopic analysis (e.g., Refs. [106,107]). Fractionation has been reported in the case of complex hydrocarbons or hydrocarbon mixtures [55], or hydrous pyrolysis [54], and would also be expected for incomplete conversion, all of which can introduce systematic fractionation in some components. This was observed in our experimental data, although the apparent isotopic fractionations imposed were much less for carbon-bound hydrogen reactions than for water splitting, an observation made previously by Luo et al. [71].

Based on these findings, and the associated reaction mechanisms, useful constraints on the anticipated δ^2H range for methane pyrolysis were made (Fig. 3a) assuming produced H_2 will largely mimic the known range of carbon-bonded hydrogen in methane sources (Fig. 3b). Similar constraints can be placed on H_2 produced through SMR (Fig. 3a), which would be expected to lie between the global ranges of carbon-bonded hydrogen in methane and hydrogen in meteoric water (Fig. 3b). For calculations, the global ranges for biogenic and thermogenic methane were taken from Schoell [89] and global ranges for meteoric water were taken from GNIP [32]. Our experimental results for methane pyrolysis and SMR, albeit limited, fall within the predicted ranges for methane pyrolysis and SMR (see cross hatched bars, Fig. 3a). Similar ranges are expected to apply for all fossil fuel conversion methods derived from carbon-bound hydrogen. Overall, we suggest that the isotopic distinction between *grey/turquois* and *green* hydrogen derives from the fact that the latter does not utilize carbon-bound hydrogen but rather involves water splitting via physical, chemical or enzymatic mediation.

An important example was found in the literature of a commercial scale SMR that was purpose-built to include heavy-water enrichment capability using catalytic exchange [35]. Of particular importance for our study, Spagnolo et al. [35] also provided isotopic data for SMR reactants and products. The setup involved two stages: (i) a primary SMR, and (ii) a secondary catalytic bed reactor. The first stage of the SMR process utilized methane feedstock containing 100 ppm deuterium (D) (δ^2H = −358 ‰) and water containing 150 ppm D (δ^2H = −37 ‰) resulting in a H_2 product with an intermediate isotopic composition (125 ppm D or δ^2H = −197 ‰). Subsequently, hydrogen produced from the SMR was directed to flow through a liquid phase catalytic exchange (LPCE) column countercurrent to liquid water being fed to the SMR, allowing the liquid water to become enriched as it flows down the exchange column. A small fraction of liquid extracted from the bottom of the LPCE column (6000 ppm D or 0.6%) was then sent for subsequent processing for further enrichment to reactor grade D_2O. Based on the plant capacity of about 23 million m^3/year of produced hydrogen, and annual output of 1 m^3 D_2O, we estimate that the produced hydrogen was likely to be altered in isotopic composition by about −500‰ through the catalytic exchange process. Although this required significant modifications to the SMR to reduce reformer losses of hydrogen-containing species to well below normal SMR standards [35], we acknowledge that introduction of catalytic exchangers to SMR could potentially lead to isotopic signatures in the same range as *green* hydrogen. However, economic viability of operating an SMR for this purpose other than for production of D_2O is questionable, although it should be mentioned as a potential means of adulteration of the isotopic fingerprints. It is important to consider that D_2O serves an essential role for the nuclear energy industry including both fission and fusion reactors, which provide a clean source of electricity and potentially can be used to produce *pink*, *purple* and *red* hydrogen (Fig. 1). Overall, since production of D_2O is regarded expensive to implement, and while it is a highly valued commodity, it is already highly regulated, it is not likely to be a widespread confounding factor for isotopic fingerprinting of produced hydrogen.

It should be mentioned that isotopes of hydrogen have also proven useful for investigating the specific reaction mechanisms of methane conversion including the role of catalysts [[51,52,54–56]], although the majority of such experiments are carried out using labelled compounds.

3.7. Biogas and biohydrogen

Biogas, primarily a mixture of CH_4 and CO_2 and associated trace

gases such as H_2S H_2, N_2, NH_3, H_2O and O_2, is commonly produced by the anerobic decomposition of organic matter such as animal waste, sewage treatment plants, industrial wastewater, food scraps, or landfill [[108,109]]. Biogas has been promoted in some jurisdictions as a renewable feedstock for hydrogen production whereby methane is normally converted to hydrogen by a conversion process such as SMR, partial oxidation, ATR, gasification or other technology [110]. Bakkaloglu et al. [111] reported isotopic signatures for biogas methane from a variety of sources including from biogas plants (−314.4 ± 23 ‰), landfills (−268.2 ± 2.1 ‰), and sewage treatment plants (−303.9 ± 22 ‰). Overall, δ^2H in biogas methane was found to range from −341 to −267 ‰, averaging −300 ± 25 ‰ including sites in the UK, Europe, and North America. Similarly, Sherwood et al. [112] carried out a global survey of waste generated methane sources to the atmosphere and found that they ranged from −312 to −281 ‰, consistent with Bakkaloglu et al. [111]. We note that these isotopic signatures fall within the range reported by Schoell [93] for biogenic methane, and once reformed to hydrogen, would likely yield isotopic signatures in the lower range we report for SMR.

In contrast, biohydrogen is produced through fermentation and N_2 fixation in algae, microalgae or bacteria using two key metal enzymes, nitrogenase and hydrogenase [24]. Very depleted isotopic signatures have been reported for nitrogen fixation from the oceans [59,61,63,75,94]; nitrogen fixation from land surfaces [59,62,75], nitrogenase/hydrogenase sources generated by cyanobacteria [67], and from a biohydrogen plant [70]. The magnitude of the isotopic fractionation has been noted to be similar to that calculated for hydrogen ions in equilibrium with water [34], and significantly larger than reactions that reform carbon-bound hydrogen [71]. Bottinga [34] showed an increase with temperature in the isotopic separation between water and produced hydrogen at equilibrium, which was confirmed by Walter et al. [70]. This isotopic offset is be expressed as:

$$1000 \ln \alpha_{H2-H2O} \simeq \varepsilon_{H2-H20} \simeq \delta_{H2} - \delta_{H20} \ (‰)$$

where $\alpha_{H2-H2O} = R_{H2}/R_{H2O}$ is the equilibrium fractionation factor, R_x corresponding to the isotopic ratio ($^2H/^1H$) in the specified sample x. As defined by Fritz and Fontes [113], the isotopic separation factor $\varepsilon_{H2\text{-}H20}$ is a close approximation of 1000ln α_{H2-H2O} and the delta value difference between the components, in this case H_2 being heavy-isotope depleted relative to H_2O such that $\alpha_{H2-H2O} < 1$ and $\varepsilon_{H2\text{-}H20} < 0$. The global average $\varepsilon_{H2\text{-}H20}$ from biological sources was estimated to be −731 ‰ (±20 ‰) at 20 °C [70], which is close to the theoretical value predicted by Bottinga [34]. For the ocean study, Walter et al. [94] applied a Keeling plot approach to distinguish the isotopic signature of H_2 due to nitrogen fixation from other sources. From over 400 samples on 5 cruises, they estimated δ^2H values of −629 ‰ (±54 ‰). Unlike production of hydrogen through reforming of biogas methane, which involves restructuring carbon-hydrogen bonds, biohydrogen can be viewed rather as enzymatic water splitting. As such, it has an isotopic signature similar to hydrogen formed from other water splitting methods such as electrolysis.

3.8. Water splitting methods

Several technologies have been developed for water splitting including electrolysis, thermochemical water splitting and photocatalysis, distinguished mainly by energy sources used to overcome the highly endothermic water dissociation reaction. Electrolysis involves use of electrical currents [105], thermochemical involves use of high temperatures (500°-2000 °C) combined with chemical compounds such as cerium oxide or copper chloride [1], whereas photocatalysis is solar-driven, often using a semi-conductor catalyst [114]. Due to the similarity of these water splitting reactions (see Table 1) as well as similarity to biohydrogen, which is enzymatic water splitting, we anticipated similar depleted isotopic signatures for the produced hydrogen. Our hypothesis was confirmed by the extreme depletion observed for produced hydrogen in our electrolysis experiments (Table 2) which suggests systematic preferential transfer of the light isotopic species from the dissolved water phase to the gas phase. One experiment conducted offsite by a confidential commercial operator who provided us a sample yielded anomalously enriched H_2 for an electrolysis product (−71 ‰) which does not fit with our hypothesis regarding the large fractionations accompanying water splitting. Unfortunately, we were unable to acquire a detailed description of the apparatus used or any explanation as to why this result may have been unique. We were also unable to carry out a repeat test. We included this result in Fig. 3a but not in the statistical treatment of the results as noted previously (Table 3).

3.9. Other processes

Atmospheric processes have a large influence on the isotopic composition of hydrogen in the troposphere and stratosphere, both of which have been shown to have moderate to extreme enrichment due to complex processes involving methane and VOC oxidation, methoxyl radicals and complicated reaction pathways by which formaldehyde is converted to hydrogen gas (see Ref. [66]). Tropospheric, and above all, stratospheric hydrogen, are the most isotopically enriched hydrogen stores on Earth, ranging from +150 to +420 ‰ in δ^2H (Fig. 3b). We postulate that such reactions may be natural, low-pressure analogues for hydrogen production by partial oxidation of methane, which would suggest enriched hydrogen outputs compared to fossil fuel precursors. However, this remains to be tested.

The effect of fossil fuel combustion efficiency (shift towards heavier isotopic signature with decreased efficiency) and catalytic conversion (shift towards heavier isotopic signature with pre-catalytic conversion) on produced hydrogen signatures is also an interesting result from previous studies, as shown in Fig. 3b. Combustion efficiency was evaluated quantitatively based on availability of O_2, reaction temperature and other factors, which determined the relative mixing ratios of CO and CO_2, where efficient combustion was considered to occur when CO/CO_2 was below 8% [62]. While such effects do not appear to overwhelm the primary isotopic fingerprints, these processes appear to affect produced hydrogen signatures by controlling the degree of influence of secondary sources of hydrogen, including minor or trace amounts of atmospheric moisture. We postulate that isotopic fingerprints may also be sensitive as indicators of conversion efficiency and/or effectiveness of catalytic conversion, which could be a useful metric for process control and monitoring.

3.10. Apparent isotopic separations

A summary of apparent isotopic separation factors ε_{H2-H2O} from selected hydrogen production methods is provided in Table 5. While approximate, this summary emphasizes the reduced offsets associated with carbon-bound hydrogen reactions and larger offsets characteristic of water splitting reactions including electrolysis and biohydrogen. We reiterate that the large apparent fractionations associated with the water splitting reactions are reflective of values predicted for hydrogen ions at equilibrium with water as calculated by Bottinga [35].

3.11. Potential applications to the hydrogen economy

This compilation contributes to the explanation and better understanding of systematic differences in the hydrogen isotopic composition of produced hydrogen according to mode of production and other controls including the isotopic composition of precursors and whether or not the hydrogen is produced through carbon-bound hydrogen reactions or water splitting reactions. Given the significant distinction noted between *green* hydrogen and *grey* hydrogen, and sensitivity to factors controlling the conversion process to hydrogen, we can postulate several

Table 5
Summary of apparent isotopic separation factors observed for carbon-bound hydrogen production versus water splitting reactions.

Hydrogen type	Precursors main, *secondary*	Apparent isotopic separation[a] $\varepsilon_{H2\text{-precursor}}$ (‰ V-SMOW)
Carbon-bound hydrogen reactions		
Biomass combustion	Bulk biomass, *plant moisture, atmos. Moisture*	−128
Car exhaust- pre-catalytic	gasoline, *atmos. moisture*	−66
Car exhaust-post-catalytic	gasoline, *atmos. moisture*	−183
Fossil fuel combustion	fossil fuel, *atmos. moisture*	−68
Methane pyrolysis	methane, *atmos. moisture*	−78
Steam methane reform	methane, *feedwater*	+40
Water-splitting reactions		
Biohydrogen	incubation water, *atmos. moisture*	−689
Electrolysis	feedwater, *atmos. moisture*	−639

[a] relative to main precursor.

potential applications to the hydrogen economy.

- We anticipate that isotope fingerprinting may be useful for tracing the source and mode of formation of produced hydrogen including identification and grading of low carbon intensity (CI) products, which could be applied as a regulatory tool. Identification and certification of *green* hydrogen products that might be preferred for some users or by some political jurisdictions could support higher pricing for such low CI products.
- It is likely that isotope signatures could be applied to monitor hydrogen production processes to detect changes in efficiency, catalytic performance or other operating conditions. For regulatory purposes, individual operators could be monitored to ensure that licensed production methods are adhered to, and that feedstocks and production conditions remain consistent over time within specified thresholds.
- Mixing of specific hydrogen sources could be monitored within distribution networks to permit mass balance of various sources including leakages and degradation due to interaction with pipeline or storage infrastructure.
- Isotopic characterisation of production sources and distribution would also allow for robust tracking and mass balance of leakage impacts on the atmospheric H_2 cycle.
- Isotopic fingerprints could be used to track interactions between produced hydrogen in underground storage including hydrogeochemical interactions with geologic strata and leakage detection (e.g., Refs. [73,115]).
- Enhanced fingerprinting potential beyond simple $^2H/^1H$ ratios using clumped isotopes of hydrogen [[80,81]] offers considerable potential for future improvements to the isotope technique, especially for establishing temperature of molecular hydrogen formation in natural geologic settings. Using high-precision isotope ratio mass spectrometry, the method relies on determining variations in the proportion of doubly-deuterated molecular hydrogen isotopologues ($^2H^2H$ or DD) in addition to $^2H/^1H$ ratios, providing a second measure of sample differentiation.
- Similar use of carbon, oxygen, nitrogen and sulfur isotope signatures would aid in monitoring and understanding the fate of carbon materials both during production of *aqua*, *blue* and *turquoise* hydrogen, and related to CCUS.

4. Concluding comments

A literature review supplemented by experimental investigations establishes a first baseline for evaluating the hydrogen isotope signatures of produced hydrogen and its precursors, which may have important applications to regulation of the hydrogen economy.

Produced hydrogen carries with it the isotopic fingerprints of its mode of origin which can be readily applied, for example, to distinguish *green* and *grey* hydrogen sources. Accordingly, it may be a useful regulatory tool for the hydrogen economy.

Hydrogen production can be monitored at source or within distribution networks to quantitatively monitor variations in mode of hydrogen production.

Isotopic fingerprints are difficult and costly to adulterate. While heavy water enrichment is one method that can be used to modify isotopic fingerprints, it is already a closely regulated activity in most jurisdictions.

Preliminary investigations have shown that hydrogen may be highly reactive in some underground storage environments. Hydrogen isotopes may be a useful tool for investigating the feasibility of underground storage including the effect of hydrogeochemical interactions between stored hydrogen and the surrounding geologic environment.

Other isotopic tracers especially carbon-13 may be applied to better understand and quantify the fate of carbon left behind in the process of clean hydrogen production. This may be one strategy to improve overall management of GHG mitigation measures including CCUS.

Future research will include an operator-blind comparative study to further characterize the isotope fingerprints of an array of produced hydrogen sources in relation to basic isotopic controls including geographic area, process, reactants, products, and catalysts.

Declaration of competing interest

The authors declare that they have no known competing financial interests or personal relationships that could have appeared to influence the work reported in this paper.

Acknowledgements

We are grateful to A. Najafi, V. Chernyak, F. Sharif, M. Perez, T. Sirbu (InnoTech Alberta, Calgary) for access to facilities and assistance with the experimental work, and M. Huard (InnoTech Alberta, Edmonton) for business development leadership. Funding was provided through strategic investment grants from InnoTech Alberta. We also wish to thank a commercial gas service company for providing metadata and samples for isotopic analysis. They asked to remain anonymous.

Appendix A. Supplementary data

Supplementary data to this article can be found online at https://doi.org/10.1016/j.ijhydene.2024.04.077.

References

[1] Balat M. Possible methods for hydrogen production. Energy Sources, Part A Recovery, Util Environ Eff 2008;31:39–50. https://doi.org/10.1080/15567030701468068.
[2] Miljanic SS, Maksic A, Lausevic Z. Isotope effects in: a) catalytic generation of hydrogen from tetrahydridoborate and b) oxidation of hydrogen in fuel cells. CI&CEQ1 2005;3:124–8.
[3] International Energy Agency (IEA). Hydrogen projects database. https://www.iea.org/product/download/016382-000300-016382. [Accessed 1 March 2024].
[4] U.S. Department of Energy. U.S. National clean hydrogen strategy and Roadmap, June 2023. Accessed online 15 Dec 2023 at: https://www.hydrogen.energy.gov/docs/hydrogenprogramlibraries/pdfs/us-national-clean-hydrogen-strategy-roadmap.pdf; 2023.
[5] Natural Resources Canada. Hydrogen strategy for Canada, Dec 2020. https://natural-resources.canada.ca/sites/nrcan/files/environment/hydrogen/NRCan_Hydrogen-Strategy-Canada-na-en-v3.pdf. [Accessed 15 December 2023].
[6] U.S. Environmental Protection Agency Regulation 40 CFR Part 98, Greenhouse Gases Reporting Program Implementation. Last accessed online 6 March 2024 at: https://www.epa.gov/sites/default/files/2014-09/documents/ghgfactsheet.pdf.
[7] U.S. Department of Energy Regulation IIJA Sec 40315 (Sec 822 of EPACT-2005) in U.S. National Clean Energy Strategy and Roadmap, Table 2, p. 64. Last

accessed online 6 March 2024 at: https://www.hydrogen.energy.gov/docs/hydrogenprogramlibraries/pdfs/us-national-clean-hydrogen-strategy-roadmap.pdf.
[8] Li C, Yu C, Slen S. Isotopic studies on the mechanism of partial oxidation of CH_4 to syngas over a Ni/AL_2O_3 catalyst. Catal Lett 2001;75:183–9.
[9] Ehleringer JR, Thompson AH, Podlesak DW, Bowen GJ, Chesson LA, Cerling TE, Schwarcz H. A framework for the incorporation of isotopes and isoscapes in geospatial forensic investigtions. In: West JB, Bowen GJ, Dawson TE, Tu KP, editors. Iso-scapes: understanding, movement, pattern, and process on earth through isotope mapping. Dordrecht: Springer; 2010. p. 357–87.
[10] Meier-Augenstein W. Forensic stable isotope signatures: comparing, geo-locating, detecting linkage. WIREs Forensic Science 2019;1:e1339. https://doi.org/10.1002/wfs2.1339.
[11] Gregorčič HS, Potočnik D, Camin F, Ogrinc N. Milk authentication: stable isotope composition of hydrogen and oxygen in milks and their constituents. Molecules 2020;25:4000. https://doi.org/10.3390/molecules25174000.
[12] Kelly SD, Abrahim A, Rinke P, Cannavan A. Detection of exogenous sugars in pineapple juice using compound-specific stable hydrogen isotope analysis. NPJ Sci Food 2021;5(1):10. https://doi.org/10.1038/s41538-021-00092-5.
[13] Gat JR. Isotope hydrology: a study of the water cycle. In: Bell JNB, editor. Series on environmental science and management, vol. 6. London: Imperial College Press; 2010. p. 189.
[14] Whiticar MJ, Faber E, Schoell M. Biogenic methane formation in marine and freshwater environments: CO2 reduction vs. acetate fermentation – isotope evidence. Geochem Cosmochim Acta 1986;50:693–709.
[15] Zachleder V, Vítová M, Hlavová M, Moudříková Š, Mojzeš P, Heumann H, Becher JR, Bišová K. Stable isotope compounds - production, detection, and application. Biotechnol Adv 2018;36:784–97. https://doi.org/10.1016/j.biotechadv.2018.01.010.
[16] Hoefs J, Harmon R. The Earth's atmosphere – a stable isotope perspective and review. Appl Geochem 2022;143:105355. https://doi.org/10.1016/j.apgeochem.2022.105355.
[17] Milkov AV. Molecular hydrogen in surface and subsurface natural gases: abundance, origins and ideas for deliberate exploration. Earth Sci Rev 2022;230:104063. https://doi.org/10.1016/j.earscirv.2022.104063.
[18] Ogawa R, Tanii R, Dawson R, Matsushima H, Ueda M. Deuterium isotope separation by combined electrolysis fuel cell. Energy 2018;149:98–104. https://doi.org/10.1016/j.energy.2018.02.014.
[19] Wang H, Au C. Deuterium isotope effects in methane partial oxidation to syngas. Chin Sci Bull 1997;42:566–70.
[20] Newsome DS. The water-gas shift reaction. Catal Rev Sci Eng 1980;21:275–318. https://doi.org/10.1080/03602458008067535.
[21] Msheik M, Rodat S, Abanades S. Methane cracking for hydrogen production: a review of catalytic and molten media pyrolysis. Energies 2021;14:3107. https://doi.org/10.3390/en14113107.
[22] Diab J, Fulcheri L, Hessel V, Rohani V, Frenklach M. Why turquoise hydrogen will be a game changer for the energy transition. Int J Hydrogen Energy 2022;47:25831–48. https://doi.org/10.1016/j.ijhydene.2022.05.299.
[23] Sanchez-Bastardo N, Schlogl R, Ruland H. Methane pyrolysis for CO_2-free H_2 production: a green process to overcome renewable energies. Chem Ing Tech 2020;92:1596–609. https://doi.org/10.1002/cite.202000029.
[24] Xuan J, He L, Wen W, Feng Y. Hydrogenase and nitrogenase: key catalysts in biohydrogen production. Molecules 2023;28:1392. https://doi.org/10.3390/molecules28031392.
[25] Arcos JMM, Santos DMF. The hydrogen color spectrum: techno economic analysis of the available technologies for hydrogen production. Gases 2023;2023:25–46. https://doi.org/10.3390/gases3010002.
[26] Yu M, Wang K, Vredenburg H. Insights into low-carbon hydrogen production methods: green, blue and aqua hydrogen. Int J Hydrogen Energy 2021;46:21261–73.
[27] Bertagni MB, Pacala SW, Paulot F, Porporato A. Risk of the hydrogen economy for atmospheric methane. Nat Commun 2022;13:7706. https://doi.org/10.1038/s41467-022-35419-7.
[28] Dolgikh VD, Pahin AV, Mikheeva GV, Golovanova TN, Kudinov IV. Experimental research of the process of methane pyrolysis in a layer of liquid tin aiming to get hydrogen. IOP Conf Ser Earth Environ Sci 2022;1070:012017. https://doi.org/10.1088/1755-1315/1070/1/012017.
[29] Liu Z, Sajjad SD, Gao Y, Yang H, Kaczur JJ, Masel RI. The effect of membrane on an alkaline water electrolyzer. Int J Hydrogen Energy 2017;42:29661–5. https://doi.org/10.1016/j.ijhydene.2017.10.050.
[30] Brand WA, Avak H, Seedorf R, Hofmann D, Conrad TH. New methods for fully automated isotope ratio determination from hydrogen at the natural abundance level. Isot Environ Health Stud 1996;32:263–73.
[31] Coplen TB. New guidelines for reporting stable hydrogen, carbon, and oxygen isotope-ratio data. Geochem Cosmochim Acta 1996;60:3359–60. https://doi.org/10.1016/0016-7037(96)00263-3.
[32] International Atomic Energy Agency (IAEA). Global network of isotopes in precipitaiton (GNIP). available online at: https://www.iaea.org/services/networks/gnip. [Accessed 4 January 2024].
[33] Gibson JJ, Birks SJ, Edwards TWD. Global prediction of δ_A and δ^2H-$\delta^{18}O$ evaporation slopes for lakes and soil water accounting for seasonality. Global Biogeochem Cycles 2008;22:GB2031. https://doi.org/10.1029/2007GB002997.
[34] Bottinga Y. Calculated fractionation factors for carbon and hydrogen isotope exchange in the system calcite-carbon dioxide-graphite-methane-hydrogen-water vapour. Geochem Cosmochim Acta 1969;33:49–64.
[35] Spagnolo DA, Boniface HA, Sadhankar RR, Everatt AE, Miller AI, Bouin J. Prototype CIRCE plant-industrial demonstration of heavy-water production from a reformed hydrogen source. Atomic Energy of Canada Ltd , Chalk River Ontario; 2002. Technical Report AECL-12145.
[36] Wilberg KB. The deuterium isotope effect. Chem Rev 1955;55:713–43. https://doi.org/10.1021/cr50004a004.
[37] Westheimer FH. The magnitude of the primary kinetic isotope effect for compounds of hydrogen and deuterium. Chem Rev 1961;61:265–73.
[38] Horibe Y, Craig H. D/H fractionation in the system methane-hydrogen-water. Geochem Cosmochim Acta 1995;24:5209–17.
[39] Roy LP. Influence of temperature on the electrolytic separation factor of hydrogen isotopes. Can J Chem 1962;40:1452–60.
[40] Wicke E. Isotope effects in palladium-hydrogen systems: the concentration of deuterium and tritium. Platin Met Rev 1971;15:144–6.
[41] Ivanchuck OM, Goryanina VG, Rozenkevich MB. Isotopic effects of hydrogen during the decomposition of water in electrolysis with a solid polymer electrolyte. Atom Energy 2000;89:745–9.
[42] Sato H, Matsushima H, Ueda M, Ito H. Effect of water stoichiometry on deuterium isotope separation by anion exchange membrane water electrolysis. Int J Hydrogen Energy 2021;46:33689–95. https://doi.org/10.1016/j.ijhydene.2021.07.202.
[43] Xue X, Zhang M, Wei F, Liang C, Liang J, Li J, Cheng W, Deng K, Liu W. Gold as an efficient hydrogen isotope separation catalyst in proton exchange membrane water electrolysis. Int J Hydrogen Energy 2022;47:26842–9. https://10.1016.j.ihydene.2022.092.
[44] Furusawa K, Nago T, Ueda M, Matsushima H. Effect of water vapor on deuterium separation by a polymer electrolyte fuel cell. Int J Hydrogen Energy 2022;47:36248–53. https://doi.org/10.1016/j.ijhydene.2022.08.188.
[45] Yasuda S, Matsushima H, Harada K, Tanii R, Terasawa T, Yano M, Asaoka H, Gueriba JS, Diño WA, Fukutani K. Efficient hydrogen isotope separation by tunneling effect using graphene-based heterogeneous electrocatalysts in electrochemical hydrogen isotope pumping. ACS Nano 2022;16:14362–9. https://doi.org/10.1021/acsnano.2c04655.
[46] Harada K, Tanaii R, Matsushima H, Ueda M, Sato K, Haneda T. Effects of water transport on deuterium isotope separation during polymer electroyte membrane water electrolysis. Int J Hydrogen Energy 2020;45:31389–95. https://doi.org/10.1016/j.ijhydene.2020.08.256.
[47] Yanase S, Oi T. H/D isotope effects accompanying electrolysis of water as studied by molecular orbital calculations. J Comput Chem Jpn 2011;2:69–74. https://doi.org/10.2477/jccj.H2302.
[48] Yanase S, Oi T. Density functional theory calculations of H/D isotope effects on polymer electrolyte membrane fuel cell operations. Z Naturforsch 2015;2015:429–35. https://doi.org/10.1515/zna-2015-0009.
[49] Galley MR. Future trends in heavy water production. Technical report AECL-7547, fourth pacific basin conference, Vancouver 11-15 September 1983. Chalk River Ontario: Atomic Energy of Canada Ltd; 1983. p. 18.
[50] U.S. Department of Commerce. Control of deuterium that is intended for use other than in a nuclear reactor under the Export Administration Regulations (EAR). Bureau of Industry and Security, 16 CFR Part 774, RIN 0694–AI44, Federal Register 2021;86(191):55492.
[51] Hu YH, Feeley JS. Thermodynamic isotope effect in partial oxidation of methane to syngas. AIChE J 2003;49:3253–9.
[52] Hu Y, Ruckenstein E. Isotopic GCMA study of the mechanism of methane partial oxidation to synthesis gas. J Phys Chem A 1998;102:10568–71. https://doi.org/10.1021/jg9837535.
[53] Yanase S, Oi T. Observations of H/D isotope effects on polymer electrolyte membrane fuel cell operations. J Nucl Sci Technol 2013;50:808–12. https://doi.org/10.1080/00223131.2013.800810.
[54] He K, Zhang S, Mi J, Zhang W. Pyrolysis involving n-hexadecane, water and minerals: insight into the mechanisms and isotope fractionation for water-hydrocarbon reaction. J Anal Appl Pyrol 2018;130:198–208. https://doi.org/10.1016/j.jaap.2018.01.009.
[55] Lui Q, Pend W, Meng Q, Zhu D, Jin Z, Wu X. Fractionation of carbon and hydrogen isotopes of TSR-altered gas products under closed system pyrolysis. Sci Rep 2020;10:12921. https://10.1038/s41598-020-69580-0.
[56] Mao X, Hu X, Cui W, Matsuura H, Tsukihasa F, Chou K. Study of hydrogen production kinetics using isotope exchange method. Int J Hydrogen Energy 2023;48:37708–14. https://doi.org/10.1016/j.ijhydene.2022.07.225.
[57] Rahn T, Eiler JM, Boering KA, Wennberg PO, McCarthy MC, Tyler S, Schauffler S, Donnelly S, Atlas E. Extreme deuterium enrichment in stratospheric hydrogen and the global atmospheric budget of H_2. Nature 2003;424:918e921. https://doi.org/10.1038/nature01917.
[58] Batenburg AM, Walter S, Pieterse G, Levin I, Schmidt M, Jordan A, et al. Temporal and spatial variability of the stable isotopic composition of atmospheric molecular hydrogen: observations at six EUROHYDROS stations. Atmos Chem Phys 2011;11:6985–99. https://doi.org/10.5194/acp-11-6985-2011.
[59] Rhee TS, Brenninkmeijer CAM, Röckmann T. The overwhelming role of soils in the global atmospheric hydrogen cycle. Atmos Chem Phys 2006;6:1611–25. https://doi.org/10.5194/acp-6-1611-2006.
[60] Rhee TS, Brenninkmeijer CAM, Röckmann T. Hydrogen isotope fractionation in the photolysis of formaldehyde. Atmos Chem Phys 2008;8:1353–66. https://doi.org/10.5194/acp-8-1353-2008.
[61] Price H, Jaeglé L, Rice A, Quay P, Novelli PC, Gammon R. Global budget of molecular hydrogen and its deuterium content: constraints from ground station, cruise, and aircraft observations. J Geophys Res 2007;112:D22108. https://doi.org/10.1029/2006JD008152.
[62] Röckmann T, Alvarez CX, Walter S, van der Veen C, Wollny AG, Gunthe SS, Helas G, Poschl U, Keppler F, Greule M, Brand WA. Isotopic composition of H_2

from wood burning: dependency on combustion efficiency, moisture content, and δD of local precipitation. J Geophys Res Atmos 2010;115:D17308. https://doi.org/10.1029/2009JD013188.
[63] Gerst S, Quay P. Deuterium component of the global molecular hydrogen cycle. J Geophys Res 2001;106:5021–31.
[64] Vollmer MK, Walter S, Bond SW, Soltic P, Röckmann T. Molecular hydrogen (H_2) emissions and their isotopic signatures (H/D) from a motor vehicle: implications on atmospheric H_2. Atmos Chem Phys 2010;10:5707e5718. https://doi.org/10.5194/acp-10-5707-2010.
[65] Joelsson LMT, Schmidt JA, Nilsson EJK, Blunier T, Griffith DWT, Ono S, Johnson MS. Kinetic isotope effects of $^{12}CH_3D + OH$ and $^{13}CH_3D + OH$ from 278 to 313 K. Atmos Chem Phys 2016;16:4439–49. https://doi.org/10.5194/acp-16-4439-2016.
[66] Nilsson EJK, Johnson MS, Taketani F, Matsumi Y, Hurley MD, Wallington TJ. Atmospheric deuterium fractionation: HCHO and HCDO yield in the $CH_2DO + O_2$ reactions. Atmos Chem Phys 2007;7:5873–81.
[67] Nilsson EJK, Andersen VF, Skov H, Johnson MS. Pressure dependent deuterium fractionation in the formation of molecular hydrogen in formaldehyde photolysis. Atmos Chem Phys Discuss 2009;9:24029–50.
[68] Rice AL, Quay P. Isotopic composition of formaldehyde in urban air. Environ Sci Technol 2009;43:8752–8. https://doi.org/10.1021/es9010916.
[69] Rice AL, Quay P. Isotopic analysis of atmospheric formaldehyde by gas chromatography isotope ratio mass spectroscopy. Anal Chem 2006;78:6320–6. https://doi.org/10.1021/ac0602367.
[70] Walter S, Laukenmann S, Stams AJM, Vollmer MK, Gleixner G, Röckmann T. The stable isotopic signature of biologically produced molecular hydrogen (H_2). Biogeosciences 2012;9:4115–23. https://doi.org/10.5194/bg-9-4115-2012.
[71] Luo Y-H, Sternberg L, Suda S, Kumazawa S, Mitsui A. Extremely low D/H ratios of photoproduced hydrogen by cyanobacteria. Plant Cell Physiol 1991;32:897–900.
[72] Yang H, Gandhi H, Shi L, Kreuzer HW, Ostrom NE, Hegg EL. Using gas chromatography/isotope ratio mass spectrometry to determine the fractionation factor for H_2 production by hydrogenases. Rapid Commun Mass Spectrom 2012;26:61–8. https://doi.org/10.1002/rcm.5298.
[73] Loffler M, Schrader M, Luders K, Werban U, Hornbruch G, Dahmke A, Vogt C, Richnow HH. Stable hydrogen isotope fractionation of hydrogen in a field injection experiment: simulation of a gaseous H_2 leakage. ACS Earth Space Chem 2022;6:631–41. 10.1021.acsearthspacechem.1c00254.
[74] Mar KA, McCarthy MC, Connell P, Boering KA. Modeling the photochemical origins of the extreme deuterium enrichment in stratospheric H_2. J Geophys Res 2007;112:D19302. https://doi.org/10.1029/2006JD007403.
[75] Pieterse G, Krol MC, Batenburg AM, Steele LP, Krummel PB, Langenfelds RL, Röckmann T. Global modelling of H_2 mixing ratios and isotopic compositions with the TM5 model. Atmos Chem Phys 2011;11:7001–26.
[76] Li S, Mosier D, Kouris A, Humez P, Mayer B, Strous M, Diao M. High diversity, abundance and expression of hydrogenases in groundwater. bioRxiv 2023;10(3):560699. https://doi.org/10.1101/2023.10.03.560699. 2023.
[77] Lin L-H, Hall J, Lippmann-Pipke J, Ward JA, Sherwood Lollar B, DeFlaun M, et al. Radiolytic H_2 in continental crust: nuclear power for deep subsurface microbial communities. G-cubed 2005;6:1–13. https://doi.org/10.1029/2004GC000907.
[78] Lin L-H, Slater GF, Sherwood Lollar B, Lacrampe-Couloume G, Onstott TC. The yield and isotopic composition of radiolytic H_2, a potential energy source for the deep subsurface biosphere. Geochem Cosmochim Acta 2005;69:893–903. https://doi.org/10.1016/j.gca.2004.07.032.
[79] Zgonnik V. The occurrence and geoscience of natural hydrogen: a comprehensive review. Earth Sci Rev 2020;203:103140. https://doi.org/10.1016/j.earscirev.2020.103140.
[80] Popa ME, Paul D, Janssen C Röckmann. H_2 clumped isotope measurements at natural isotopic abundances. Rapid Commun Mass Spectrom 2019;33:239–51. https://doi.org/10.1002/rcm.8323.
[81] Mangenot X, Xie H, Cremiere A, Glunta T, Lilley M, Sissmann O, Orphan V, Schimmelmann A, Gaucher EC, Girard J-P, Eiler J. ^2H-^2H clumping in molecular hydrogen method and preliminary results. Chem Geol 2023;621:121278. https://doi.org/10.1016/j.chemgeo.2022.212278.
[82] Boreham CJ, Edwards DS, Czado K, Rollet N, Wang L, van der Wielen S, Champion D, Blewett R, Feitz A, Henson PA. Hydrogen in Australian natural gas: occurrences, sources and resources. The APPEA Journal 2021;61:163–91. https://doi.org/10.1071/AJ20044.
[83] Hallis LJ. D/H ratios of the inner solar system. Phil. Trans. R. Soc. A. 2016;375:20150390. https://doi.org/10.1098/rsta.2015.0390.
[84] Aleon J, Levy D, Aleon-Toppani A, Bureau H, Khodja H, Brisset F. Determination of the initial hydrogen isotopic composition of the solar system. Nat Astron 2022;6:458–63. https://doi.org/10.1038/s41550-021-01595-7.
[85] Lyon GL, Hulston JR. Carbon and hydrogen isotopic compositions of New Zealand geothermal gases. Geochem Cosmochim Acta 1984;48:1161–71. https://doi.org/10.1016/0016-7037(84)90052-8.
[86] Clog M, Aubaud C, Cartigny P, Dosso L. The hydrogen isotopic composition and water content of southern Pacific MORB: a reassessment of the D/H ratio of the depleted mantle reservoir. Earth Planet Sci Lett 2013;381:156–65. https://doi.org/10.1016/j.epsl.2013.08.043.
[87] Bell DR, Ihinger PD. The isotopic composition of hydrogen in nominally anhydrous mantle minerals. Geochem Cosmochim Acta 2000;64:2109–18. https://doi.org/10.1016/S0016-7037(99)00440-8.
[88] Proskurowski G, Lilley MD, Kelley DS, Olson EJ. Low temperature volatile production at the Lost City hydrothermal field, evidence from a hydrogen stable isotope geothermometer. Chem Geol 2006;229:331–43. https://doi.org/10.1016/j.chemgeo.2005.11.005.
[89] Vacquand C, Deville E, Beaumont V, Guyot F, Sissmann O, Pillot D, et al. Reduced gas seepages in ophiolitic complexes: evidences for multiple origins of the H_2-CH_4-N_2 gas mixtures. Geochem Cosmochim Acta 2018;223:437–61. https://doi.org/10.1016/j.gca.2017.12.018.
[90] Shangguan Z, Huo W. δD values of escaped H_2 from hot springs at the Tengchong Rehai geothermal area and its origin. Chin Sci Bull 2002;47:148–51.
[91] Cheng T, Changbo Z, QinQiang M, Yu Z, Huamin Y. Deuterium/hydrogen ratio analysis and characteristics of hydrogen in natural gases. Earth Environ. Sci. 2020;600:012028. https://doi.org/10.1088/1755-1315/600/1/012028.
[92] Yang X, Keppler H, Li Y. Molecular hydrogen in mantle minerals. Geochem. Perspect. Lett. 2016;2:160–8. https://doi.org/10.7185/160geochemlet.1616.
[93] Schoell M. The hydrogen and carbon isotopic composition of methane from natural gases of various origins. Geochem Cosmochim Acta 1980;44:649–61.
[94] Walter S, Kock A, Steinhoff T, Fiedler B, Fietzek P, Kaiser J, et al. Isotopic evidence for biogenic molecular hydrogen production in the Atlantic Ocean. Biogeosciences 2016;13:323–40. https://doi.org/10.5194/bg-13-323-2016.
[95] Schiegl WE, Vogel JC. Deuterium content of organic matter. Earth Planet Sci Lett 1970;7:307–13. https://doi.org/10.1016/0012-821X(69)90041-7.
[96] Douglas PMJ, Stratigopoulos E, Park S, Phan D. Geographic variability in freshwater methane hydrogen isotope ratios and its implications for global isotopic source signatures. Biogeosciences 2021;18:3505–27.
[97] O'Sullivan G, Kalin RM. Investigation of the range of carbon and hydrogen isotopes within a global set of gasolines. Environ Forensics 2008;9:166–76. https://doi.org/10.1080/15275920802119037.
[98] Schiegl WE. Deuterium content of peat as a paleoclimatic recorder. Science 1972;175:512–3.
[99] Mora G, Zanazzi A. Hydrogen isotope ratios of moss cellulose and source water in wetlands of Lake Superior, United States reveal their potential for quantitative paleoclimatic reconstructions. Chem Geol 2017;468:75–83. https://doi.org/10.1016/j.chemgeo.2017.08.017.
[100] Redding CE, Schoell M, Monin JC, Durand B. Hydrogen and carbon isotopic composition of coals and Kerogens. Phys Chem Earth 1980;12:711–23. https://doi.org/10.1016/0079-1946(79)90152-6.
[101] Ferreira AA, Santos Neto EV, Sessions AL, Schimmelmann A, Aquino Neto FR. 2H/1H ratio of hopanes, tricyclic and tetracyclic terpanes in oils and source rocks from the Potiguar Basin, Brazil. Org Geochem 2012;51:13–6. https://doi.org/10.1016/j.orggeochem.2012.07.007.
[102] Schimmelmann A, Sessions ALCJ, Edwards DS, Logan GA, Summons RE. D/H ratios in terrestrially sourced petroleum systems. Org Geochem 2004;35:1169–95.
[103] Marcano N. Isotopic and molecular studies of biodegraded oils and the development of chemical proxies for monitoring in situ upgrading of bitumen. University of Calgary; 2011. p. 368. Ph.D. Thesis.
[104] Enhalt DH, Rohrer F. The tropospheric cycle of H_2: a critical review. Tellus 2009;61B:500–35. https://doi:10.1111/j.1600-0889.2009.00416.x.
[105] Saulnier R, Minnich K, Sturgess PK. Water for the hydrogen economy. White Paper. Edmonton Canada: WaterSmart Solutions Ltd; 2020. p. 13.
[106] Sofer Z, Schiefelbein CF. Hydrogen isotope ratio determinations in hydrocarbons using the pyrolysis preparation technique. Anal Chem 1986;58:2033–6.
[107] Tobias HJ, Brenna JT. On-line pyrolysis as a limitless reduction source for high-precision isotopic analysis of organic-derived hydrogen. Anal Chem 1997;69:3148–52. https://doi.org/10.1021/ac970332v.
[108] Li Y, Phoumin h, Kimera S. Hydrogen sourced from renewables and clean energy: a feasibility study of achieving large-scale demonstration. ERIA Research Project Report 2021;19:292.
[109] Alves HJ, Junior CB, Niklevicz RR, Frigo EP, Frigo MS, Coimbra-Araujo CH. Overview of hydrogen production technologies from biogas and the application in fuel cells. Hydrogen Energy 2013;38:5215–25.
[110] Kumar R, Kumar A, Pal A. Overview of hydrogen production from biogas reforming: technological advancement. Int J Hydrogen Energy 2022;47:34831–55. https://doi.org/10.1016/j.ijhydene.2022.08.059.
[111] Bakkaloglu S, Lowry D, Fisher RE, Menoud M, Lanoisellé M, Chen H, Röckmann T, Nisbet EG. Stable isotopic signatures of methane from waste sources through atmospheric measurements. Atmos Environ 2022;276:119021. https://doi.org/10.1016/j.atmosenv.2022.119021.
[112] Sherwood OA, Schwietzke S, Arling VA, Etiope G. Global inventory of gas geochemistry data from fossil fuel, microbial and burning sources. Earth Syst Sci Data 2017;9:639–56. https://doi.org/10.5194/essd-9-639-2017.
[113] Fritz P, Fontes JCh. In: Fritz P, Fontes JCh, editors. Handbook of environmental geochemistry, Vol. 1 the terrestrial environment A, Chapter 1. Introduction. New York: Elsevier; 1980. p. 5–6.
[114] Li, Li X, Li J, Wei B. Boosting photocatalytic hydrogen production from water by photothermally induced biphase systems. Nat Commun 2021;12:1343. https://doi.org/10.1038/s41467-021-21526-4.
[115] Flesch S, Pudlo D, Albrecht D, Jacob A, Enzmann F. Hydrogen underground storage – petrographic and petrophysical variations in reservoir sandstones from laboratory experiments under simulated reservoir conditions. Int J Hydrogen Energy 2018;43:20822–35. https://doi.org/10.1016/j.ijhydene.2018.09.112.